

Seismic Performance of TMDs in Improving the Response of MRF Buildings

S.M. Zahrai* and A. Ghannadi-Asl¹

In this paper, the effectiveness of Tuned Mass Dampers (TMDs) in controlling building structures under earthquake excitations is studied through investigating the practical considerations and vibration control efficiency of tuned mass dampers for 5-, 8-, 10- and 15-story buildings utilizing a structural system with special Moment-Resisting Frames (MRFs) in both directions. Assuming its frequency to be near the 1st natural frequency of buildings, it is designed to control the largest response of the buildings. The effect of detuning, on some TMD parameters, on the seismic performance is studied through time-history analysis using the El Centro and Tabas earthquake records. In addition, the results of time-history analysis are compared with those of a response spectrum analysis for the structures with and without TMD, in order to judge its effectiveness. Under earthquake excitation, the performance of structures having TMDs greatly depends on the characteristics of the ground motion. When the first mode of a MDOF structure dominates the structural response, a seismic response reduction can be easily achieved. While the first mode response of a structure with TMD is proved to be substantially reduced, the higher mode response, in fact, increases as the number of stories increases. It is observed that TMD is effective in reducing maximum displacement in MRF buildings by as much as 32.2% in the Tabas earthquake and 45.3% in the El Centro earthquake. The maximum displacement results of a response spectrum analysis for the uncontrolled and controlled case in the El Centro earthquake, in an 8-story structure, are 25.70 cm and 14.59 cm, respectively, whereas the maximum displacement using time-history analysis, in the uncontrolled and controlled cases, are 27.54 cm and 15.14 cm, respectively.

INTRODUCTION

Through intensive research and development in recent years, the TMD has been accepted as an effective vibration control device for both new and existing structures, to enhance their reliability against wind, earthquake and human activity. TMDs can be incorporated into an existing structure with less interference compared with other passive energy dissipation devices [1]. The TMD is found to be a simple, effective, inexpensive and reliable means for suppressing undesirable vibrations of structures caused by harmonic or wind excitations [2].

The main objective of incorporating TMD is to

reduce energy dissipation demands on the structural members. This reduction is accomplished by transferring some of the structural vibrational energy to the TMD which, in the simplest form, consists of a mass, a spring and a damper, attached to the main structure [3].

The concept of vibration control, using a mass damper, dates back to the year 1909, when Frahm invented a vibration control device called a dynamic vibration absorber. Since 1971, many TMDs have been successfully installed in high-rise buildings and towers all over the world (for example, the Citicorp Center in New York City, the John Hancock Building in Boston [4], the Sydney Tower in Sydney [5], the Crystal Tower Building in Osaka and many observatory towers in Japan) and have been reported as being able to reduce wind-induced vibrations. As shown in Figure 1, TMD is a fundamental mechanism, in which understanding of TMD behavior and its design are important subjects. The vibration control device invented by Frahm did not have any inherent damping.

*. Corresponding Author, Center of Excellence for Engineering and Management of Infrastructures, School of Civil Engineering, University of Tehran, Tehran, I.R. Iran.

1. Department of Civil Engineering, University of Tehran, Tehran, I.R. Iran.

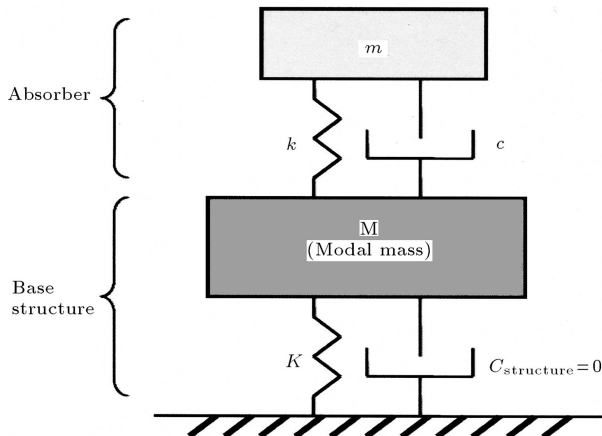


Figure 1. A schematic representation of a damped vibration absorber suggested by Den Hartog [7].

It was effective only when the absorber's natural frequency was very close to the excitation frequency and it suffered a sharp deterioration in its performance if the excitation frequency deviated from the absorber's natural frequency. In addition, if the excitation frequency approached any of the two natural frequencies of the structure-absorber system, a very large response could occur at resonance. Therefore, it was effective only for cases where the frequency of the excitation was known so that the absorber could be designed with a natural frequency equal to the excitation frequency [3,6]. This shortcoming was later eliminated when Ormondroyd and Den Hartog [7] showed that, if a certain amount of damping were introduced in Frahm's absorber, the performance deterioration, under a changing excitation frequency, would not be very sensitive and the response at resonance could also be significantly reduced.

Den Hartog also derived closed form expressions for optimum damper parameters. He assumed no damping to be present in the main mass, to facilitate the derivations. Later, damping in the main mass was included in the analysis by Bishop and Welbourn [8]. While Den Hartog considered absorbers with viscous damping only, Snowdown [9] extended it to include different types of absorber damping. Falcon et al. [10] devised a procedure for optimizing an absorber, incorporating a restricted amount of damping applied to a damped main system. Ioi and Ikeda [11] developed correction factors for the absorber parameters, as functions of the main mass damping, assuming light main mass damping. Warburton and Ayorinde [12] tabulated numerically searched optimum values of absorber parameters for certain values of the absorber to main mass ratio and main mass damping ratio. Thompson [13] presented a frequency locus method to obtain optimum damper parameters. Warburton [14] derived closed form expressions for optimum absorber parameters for undamped Single-Degree-Of-Freedom (SDOF) systems for harmonic and white noise random

excitations. Vickery et al. [15] considered a damped SDOF structure-TMD system with a TMD to main mass ratio of 5%. They developed graphs to obtain the absorber response and added effective damping, due to the absorber. Tsai and Lin [16] numerically developed plots to obtain the optimum damper parameters for harmonic excitation. They also presented empirical expression, which fit the obtained plots.

It can be generally stated that under earthquake loading, TMDs are not as effective as for wind loading, due to the following reasons:

1. The frequency bandwidth of an earthquake excitation is not only wider than that of a wind load but also, richer in high frequency content, so that high modes of a building structure are usually excited and the first mode representation of the structure is not adequate. Conventional TMD, tuned to the fundamental frequency of the structure, could suppress little or even amplify the dynamics response of higher modes and, therefore, may fail to reduce the total response under these conditions;
2. The first peak in the response history can not be easily reduced, due to the fact that TMD passively respond to the structural movement and, then, reversely mitigate the response of the structure by vibrating out-of-phase with the structural movement.

Although all TMD applications have been made towards the mitigation of wind induced motion, the seismic effectiveness of TMD has remained an important issue. While studies, to date, have not produced special results, the objective of this paper is to present the effectiveness of TMD in mitigating the seismic vibration of MRF (Moment Resisting Frame) buildings. Based on the numerical results obtained in this paper, overall, when the first mode of a MRF building dominates the structural response, a response reduction of the MRF building, using TMD under earthquake loading, can be easily achieved. On the other hand, for earthquake type excitations, the response reduction is large for resonant ground motions and diminishes as the dominant frequency of the ground motion gets further away from the structure's natural frequency to which the TMD is tuned. Therefore, it can be seen that the effect of ground motion parameters; namely, intensity of ground motion, central frequency, bandwidth of ground motion and duration of strong motion, on the seismic effectiveness of TMD and its optimum parameters, may be a problem, which needs further study.

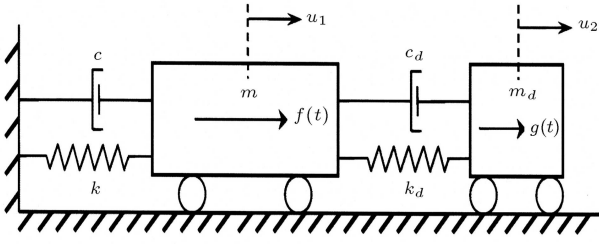


Figure 2. Model of SDOF structure and TMD.

BASIC PRINCIPLES

Consider the response of a Single-Degree-Of-Freedom (SDOF) structure-TMD system subjected to a vibratory force, $f(t)$, as shown in Figure 2. Referring to Figure 2, the equations of motion are given, as follows:

$$m\ddot{u}_1(t) + c\dot{u}_1(t) + ku_1(t) = c_d[\dot{u}_2(t) - \dot{u}_1(t)] + k_d[u_2(t) - u_1(t)] + f(t), \quad (1)$$

$$m_d[\ddot{u}_2(t) - \ddot{u}_1(t)] + c_d[\dot{u}_2(t) - \dot{u}_1(t)] + k_d[u_2(t) - u_1(t)] = -m_d\ddot{u}_1(t) + g(t), \quad (2)$$

where m is the main mass, m_d is the damper mass, k is the main spring stiffness, k_d is the absorber spring stiffness, c_d is the absorber damping, $f(t)$ is the force acting on the main mass and $g(t)$ is the force acting on the damper mass. Force acting on damper mass equals zero for wind excitation and equals $\mu \cdot f(t)$ for earthquake loading.

To facilitate further discussions, additional notations are introduced here, as follows:

$\mu, \mu = m_d/m,$	the damper mass to the main mass ratio,
ω	the frequency of a harmonic excitation,
$\omega_s, \omega_s^2 = k/m^2$	the natural frequency of the main mass,
$\omega_a, \omega_a^2 = k_d/m_d$	the natural frequency of the damper mass,
$\beta, \beta_s = \omega/\omega_s$	the ratio of excitation frequency to the main mass natural frequency,
$\alpha, \alpha = \omega_a/\omega_s$	the frequency ratio,
ξ_a	the damping ratio of TMD,
ξ_s	the damping ratio of the main mass.

Summation of Equations 1 and 2 leads to:

$$(m + m_d)\ddot{u}_1(t) + c\dot{u}_1(t) + ku_1(t) = f(t) + g(t) - m_d[\ddot{u}_2(t) - \ddot{u}_1(t)]. \quad (3)$$

It is seen that the net merger effect of the added small mass, (m_d), on the structure, aside from a slight

decrease in natural frequency and a slight increase in external force from $f(t)$ to $f(t) + g(t)$, is the addition of a force term, $[-m_d \cdot (\ddot{u}_2(t) - \ddot{u}_1(t))]$.

Once the optimal parameter values for the TMD are found, Equations 1 and 2 can be used for structural response analysis. These equations are valid only for Single-Degree-Of-Freedom (SDOF) structural systems. Since most building structures are multi-degree-of-freedom systems, a more general form of the equations of motion for a structure-TMD system (TMD is installed on top of the structure), for earthquake loading, has the following vector-matrix form:

$$m\ddot{\mathbf{u}}_1(t) + c\dot{\mathbf{u}}_1(t) + k\mathbf{u}_1(t) = c_d[\dot{\mathbf{u}}_2(t) - \dot{\mathbf{u}}_1(t)] + k_d[\mathbf{u}_2(t) - \mathbf{u}_1(t)] + \mathbf{f}(t), \quad (4)$$

$$m_d[\ddot{\mathbf{u}}_2(t) - \ddot{\mathbf{u}}_1(t)] + c_d[\dot{\mathbf{u}}_2(t) - \dot{\mathbf{u}}_1(t)] + k_d[\mathbf{u}_2(t) - \mathbf{u}_1(t)] = -m_d \cdot \frac{\boldsymbol{\varphi}^T \mathbf{M} \mathbf{r}}{\boldsymbol{\varphi}^T \mathbf{M} \boldsymbol{\varphi}} + \mathbf{g}(t), \quad (5)$$

where $\boldsymbol{\varphi}$ represents the mode shape vector. Under wind-type loading, force acting on damper mass equals zero, while, for earthquake-type excitations, force acting on damper mass equals:

$$\mathbf{g}(t) = \left(\frac{\mu}{\Gamma} \right) \cdot \mathbf{f}(t).$$

The participation factor, (Γ), is expressed as follows:

$$\Gamma = \frac{\boldsymbol{\varphi}^T \mathbf{M} \mathbf{r}}{\boldsymbol{\varphi}^T \mathbf{M} \boldsymbol{\varphi}}.$$

Den Hartog [17] developed closed form expressions of optimum damper parameters f and g which minimize the steady-state response of the main mass subjected to a harmonic excitation. For harmonic excitation with frequency ω , the static deflection is $u_{st} = P/K$, while the dynamic amplification factor for a damped structural system, DAF, is:

$$\text{DAF} = \sqrt{\frac{A^2 + B^2}{C^2 + D^2}}, \quad (6)$$

where A , B , C and D are given by:

$$A = 1 - \beta_a^2,$$

$$B = 2\xi_a\beta_a,$$

$$C = 1 - \beta_a^2 - \beta_s^2(1 + \mu) + \beta_a^2\beta_s^2 + 4\beta_a\beta_s\xi_a\xi_s,$$

$$D = 2(\beta_s\xi_s + \beta_a\xi_a) - 2\beta_a\beta_s(\beta_a\xi_s - \beta_s\xi_a(1 - \mu)).$$

Observe that the amplification factor is a function of the six essential variables: μ , ξ_a , ξ_s , α , β_s and β_a .

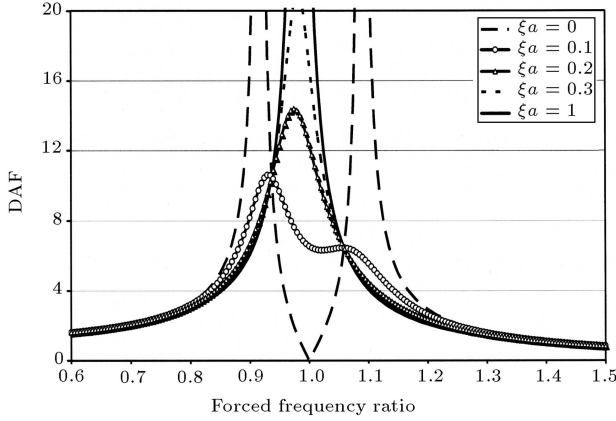


Figure 3. DAF as function of β_s .

Figure 3 shows a plot of DAF as a function of the frequency ratio, β_s , for $\alpha = 1$, $\mu = 0.03$, $\xi_s = 0$ and for various values of the TMD damping ratio.

The objective of adding the TMD is to bring the resonant peak of the amplitude down to its lowest possible value, so that smaller amplifications over a wider frequency bandwidth, with β closest to unity, can be achieved. There are two points on the DAF vs. β_s plots in Figure 3, at which DAF is independent of damping ratio, ξ_a , and the minimum peak amplitude can be obtained by first properly choosing α to adjust these two fixed points to reach equal heights. The optimum frequency ratio, α , following this procedure, is obtained, as follows:

$$\alpha_{\text{opt}} = \frac{1}{1 + \mu}. \quad (7)$$

The effect of TMD damping on the peak response of the structure is examined under an optimal frequency ratio. The damping of the structure is assumed to be negligibly small. In this case, the optimal damping, ξ_{opt} , becomes:

$$\xi_{\text{opt}} = \sqrt{\frac{3\mu}{8(1 + \mu)}}. \quad (8)$$

For the case when the structure is subjected to a harmonic base excitation, the corresponding expressions can be easily found to be:

$$\alpha_{\text{opt}} = \frac{1}{1 + \mu} \cdot \sqrt{\frac{2 - \mu}{2}}, \quad (9)$$

$$\xi_{\text{opt}} = \sqrt{\frac{3\mu}{8(1 + \mu)}} \cdot \sqrt{\frac{2}{2 - \mu}}. \quad (10)$$

Using the values of α_{opt} and ξ_{opt} , optimum values of damping c_d and stiffness k_d of the damper can be

calculated as:

$$k_d = 4\pi^2 \mu \alpha^2 \frac{m_s}{T_s^2}, \quad (11)$$

$$c_d = 4\pi \mu \alpha \xi_{\text{opt}} \frac{m_s}{T_s}. \quad (12)$$

In Den Hartog's derivation of optimal damper parameters, it is assumed that the main mass is undamped. In the presence of damping for the main mass, no closed-form expressions can be derived for the optimum damper parameters. However, they may be obtained by numerical trials with the aim of achieving a system with the smallest possible value of its higher response peak.

PHILOSOPHY OF WIDE BAND FREQUENCY TMDs

It is well known that a TMD can be designed to control a single structural mode only. Given the properties of the mode, which need to be controlled, the design problem is essentially the same as designing a TMD for a SDOF structure. Parametric studies were performed on a SDOF structure-TMD system to enhance the understanding of TMD behavior. The numerical optimization, using a minimax approach, was used for obtaining optimum TMD parameters.

A reasonable model of TMD that encompasses the TMD concept, which can operate in a wide band frequency, is considered. One element that does not show any deflection and rotation, as a support, is attached to a dashpot, spring and a mass, in such a way that only transitional constraints are satisfied. Configuration of the model is designed, so that ground motion excitation initially affects the spring-dashpot system and, therefore, TMD mass is excited with a phase delay. This performance provides appropriate movement for TMD to counteract the forces, due to the strong ground motion.

SELECTING TMD PARAMETERS FOR SEISMIC CONTROL

It is clear that, in the first mode, the top floor will undergo the largest steady-state deflection under a harmonic excitation. Under wind excitation, TMD effectiveness, when attached to one floor of a MDOF structure, is exactly the same as in the SDOF system. For earthquake excitations, when the TMD is situated at the top floor of a building structure, every element of the modal vector, φ , is less than, or equal to, unity. The participation factor, Γ , is, thus always greater than unity, which improves the effectiveness, in the sense that the effect of $g(t)$ on the damper is decreased. On the other hand, if the TMD is installed at a lower floor,

the mass ratio, μ , is reduced at a greater rate than the participation factor and, therefore, TMD effectiveness is expected to diminish. Therefore, the TMD should be placed at the top floor for best control of the first mode. If T is the first mode period of a building, a TMD, with a natural period in the range of $T - \varepsilon$ to $T + \varepsilon$, is chosen, in order to contain the effective structural mode. The optimal damping ratio of TMD is also adopted from Den Hartog recommendations [18].

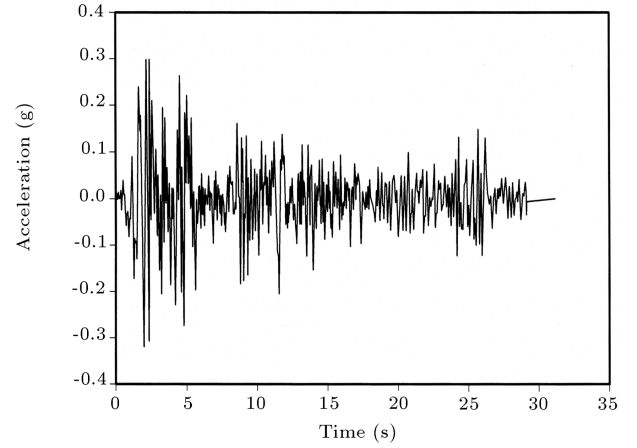
SELECTING RECORDS

Earthquakes with magnitudes of less than 5 are of minor concern for strong motion seismology. They are not known to damage modern structures. Only a tiny fraction of such small events has caused death. As the magnitude grows, both the destructive capability and average number of deaths per event also grow. Events with magnitudes between 6 and 7.5 are the most commonly responsible for significant disasters. Events with a magnitude of over 8, of course, have immense destructive potential, but fortunately they occur at an average rate of only about once per year and some are located in remote oceanic locations. Therefore, two component records selected in this study are assigned to major events with magnitudes of about 7 and, in the source distances, less than 30 km. The records are accelerographs of the Tabas and El Centro earthquakes, as shown in Figure 4.

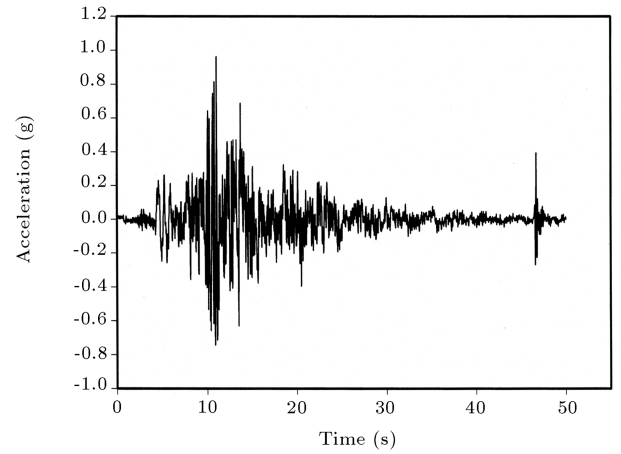
The 1978 Tabas earthquake took place on September 16 and was one of the largest earthquakes to hit Iran. The earthquake was measured at 7.4 on the Richter scale. The Tabas earthquake was registered on 11 accelerograph stations, with source distances ranging from 3 to 350 km and corresponding recorded peak accelerations ranging from 0.95 down to 0.01 g, respectively. The El Centro earthquake has been used in many previous analytical investigations. This earthquake took place on May 18 and was one of the earthquakes to hit California, measuring 7 on the Richter scale. The El Centro earthquake was registered at the Imperial Valley Irrigation District substation with an absolute peak acceleration of 0.349 g. These earthquake records are two far-fields. The Tabas and El Centro earthquakes have thrust and strike-slip mechanisms, respectively.

NUMERICAL EXAMPLES

In this study, the design of a TMD tuned to the first mode of structures, described in the previous section, is carried out under harmonic base excitation. For this purpose, a series of 5-, 8-, 10- and 15-story buildings are considered. The plan and elevation of the 8-story building are shown in Figure 5. A time-history analysis is performed on the structures considered under the El



(a) The El Centro excitation



(b) The Tabas excitation

Figure 4. The El Centro and Tabas ground excitations.

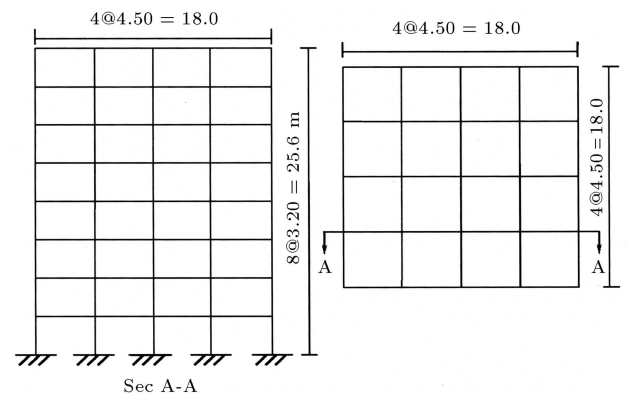


Figure 5. Section and plan views of the 8-story building.

Centro and Tabas earthquakes. Two different ground motions are employed, as the input ground motions are not scaled.

The buildings utilize a structural system with special moment-resisting frames in both directions and are designed only for gravity and wind and earthquake

loads, according to the Iranian codes [19]. A uniformly distributed live load of 200 kg/m^2 , a uniformly distributed dead load of 810 kg/m^2 and a maximum wind pressure of approximately 100 kg/m^2 (e.g., 15-story building) are assumed. The yield stress of the steel was assumed to be 240 MPa.

However, it should be noted that numerous general purpose finite element software packages currently exist to solve the structural dynamics problem, including ABAQUS, ADINA, ANSYS and MSC/NASTRAN. While none of these programs specifically address the special formulations needed to characterize passive energy dissipation devices, most permit generic user-defined elements. Alternatively, one can utilize packages geared exclusively toward civil engineering structures, such as ETABS, DRAIN and IDARC, which in some cases can already accommodate typical passive elements. Therefore, the ETABS software [20] is used to analyze and design the structures.

The fundamental periods of the structures and modal participating mass ratios, determined from analysis, are listed in Table 1. For most applications, the mass ratio is less than about 0.05. In this study, the weight of TMD is about 0.03 of the total weight of the structure. The total mass of the structures, mass m_d , stiffness k_d and damping c_d of TMDs, which are calculated based on the design method above, are listed in Table 2.

Figure 6a shows the maximum displacement time-histories of structures with and without TMD under the El Centro earthquake. It demonstrates that the maximum displacement of the top story of the uncontrolled case is 27.54 cm and that of the controlled case is 15.14 cm in an 8-story structure. In comparison with an 8-story structure, in a 10-story structure, the maximum displacement of the top story of the uncontrolled case is 39.57 cm and that of the controlled case is 24.84 cm. On the other hand, Figure 6b shows the maximum displacement time-histories of structures with and without TMD under the Tabas earthquake.

In this figure, the maximum displacement at the top story of the uncontrolled case is 34.16 cm and that of the controlled case is 25.80 cm in a 5-story structure. Whereas, in a 15-story structure, the maximum response of the top story of the uncontrolled case is 1.45 m and that of the controlled case is 1.12 m.

The effectiveness of tuned mass dampers in controlling building structures under seismic excitation is shown in Figure 7.

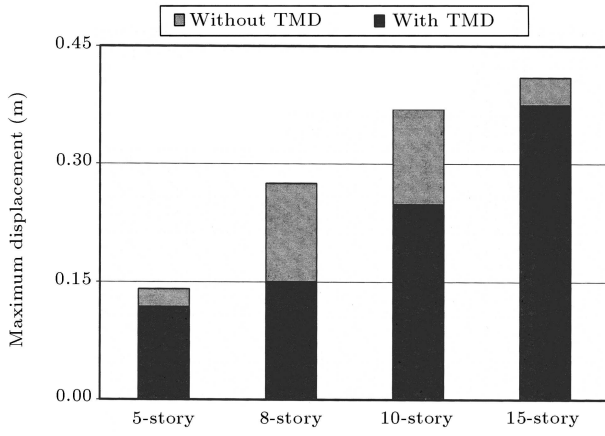
It clearly shows that TMD can reduce the maximum seismic response of structures significantly. The reduction of maximum displacement is as much as 16.6-32.2% under the Tabas earthquake and 8.6-45.3% under the El Centro earthquake. Figure 7a shows the displacement reduction of the top story in an 8-story structure by as much as 45.3% under the El Centro

Table 1. Lateral periods of the structures and modal participating mass ratios.

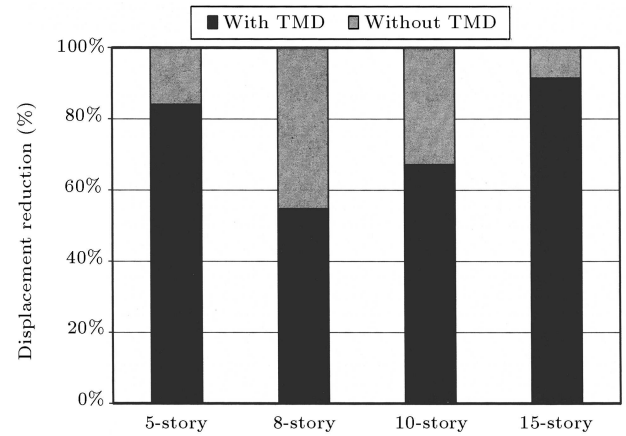
Mode No		1	2	3	4	5
5-Story	Period (s)	1.6021	0.5169	0.2825	-	-
	Modal participating mass ratio (%)	77.928	90.131	95.433	-	-
8-Story	Period (s)	2.2627	0.7840	0.4424	0.2874	-
	Modal participating mass ratio (%)	76.508	88.777	93.208	95.470	-
10-Story	Period (s)	2.6943	0.9837	0.5507	0.3690	-
	Modal participating mass ratio (%)	75.088	87.861	92.310	94.772	-
15-Story	Period (s)	3.5520	1.3370	0.7727	0.5286	0.3879
	Modal participating mass ratio (%)	72.601	86.613	91.043	93.259	94.693

Table 2. Total mass of the structures and mass of the TMD.

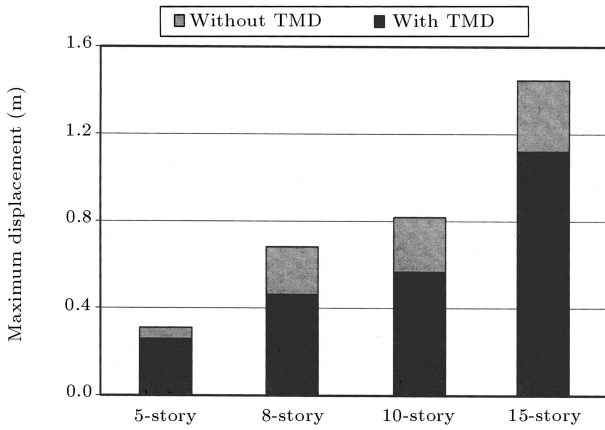
Parameters	Total Mass of the Structure (kgf)	Mass of TMD (kgf)	Stiffness of TMD (kg/m)	Damping Ratio of TMD
5-Story	149990.9	4499.727	65034.1	10.5%
8-Story	240940.4	7228.212	52006.01	10.5%
10-Story	301523.3	9045.699	46370.38	10.5%
15-Story	458546.7	13756.401	41572.99	10.5%



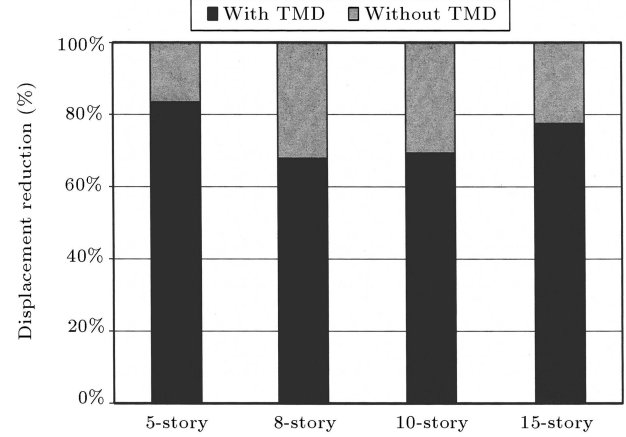
(a) Structures under the El Centro earthquake



(a) Structures under the El Centro earthquake



(b) Structures under the Tabas earthquake



(b) Structures under the Tabas earthquake

Figure 6. Maximum displacement of structures with and without TMD.

earthquake. The figure also exhibits the displacement reduction of the top story in a 10-story structure by as much as 32.9% under the El Centro earthquake, while Figure 7b presents the displacement reduction of the top story in an 8-story structure by as much as 32.2% under the Tabas earthquake. On the other hand, one can see that the displacement reduction of the top story in a 10-story structure is as much as 30.8% under the Tabas earthquake.

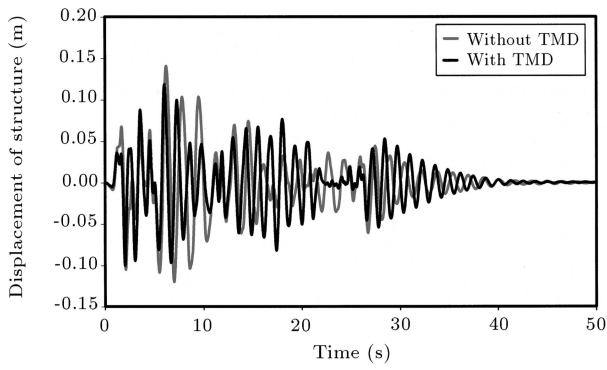
The results of time-history analysis are shown in Figures 8 to 11. These figures show the displacement and the acceleration of structures with and without TMD under the El Centro and Tabas earthquakes,

Figure 7. Maximum displacement reduction of structures.

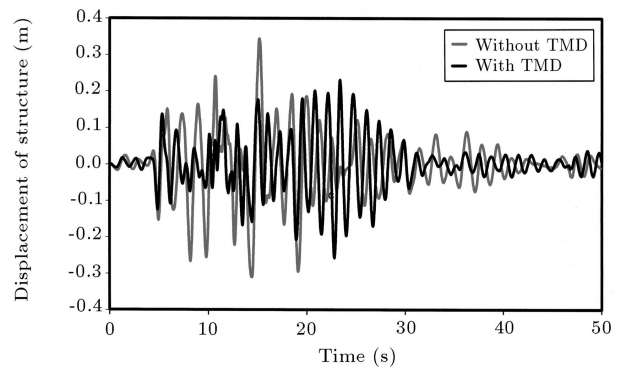
respectively. Tables 3 and 4 list the Root Mean Square (RMS) values of the displacements and the accelerations of the structures subjected to the El Centro and Tabas earthquakes, respectively. Table 3 shows much improvement in reducing the displacement of the structures, except for the RMS in a 15-story structure. Referring to Table 3 and Figure 8d, it is noticed that conventional TMD, tuned to the first mode of the structure, could suppress little or even amplify the dynamic response of higher modes and, therefore, may fail to reduce the total response under these conditions. This condition is seen in the 15-story building.

Table 3. RMS values of the displacements of the structures.

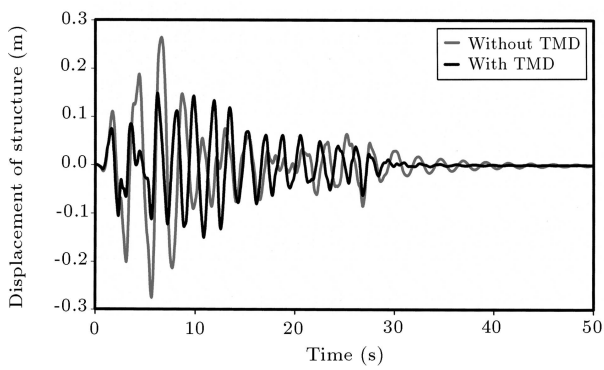
Structures	Displacements Under the Tabas (cm)			Displacements Under the El Centro (cm)		
	Uncontrolled	Controlled	<i>R</i>	Uncontrolled	Controlled	<i>R</i>
5-Story	8.92523	7.49909	0.84021	3.36297	3.10690	0.92386
8-Story	18.01218	11.44672	0.63550	6.40886	4.53289	0.70728
10-Story	22.43477	16.23178	0.72351	8.76954	5.80765	0.66225
15-Story	47.31376	28.67116	0.60598	9.96115	12.13366	1.21810



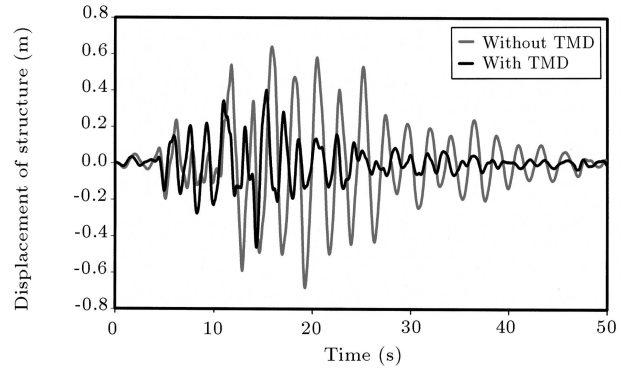
(a) 5-story structure



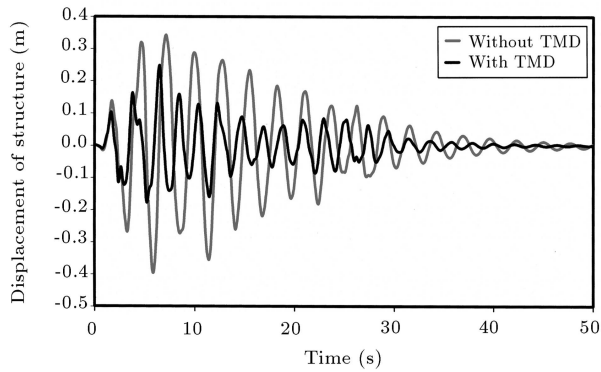
(a) 5-story structure



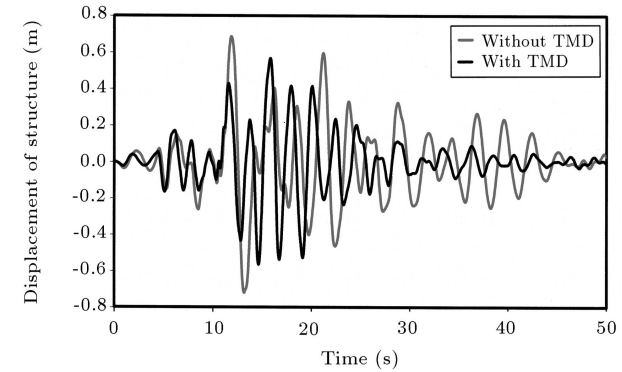
(b) 8-story structure



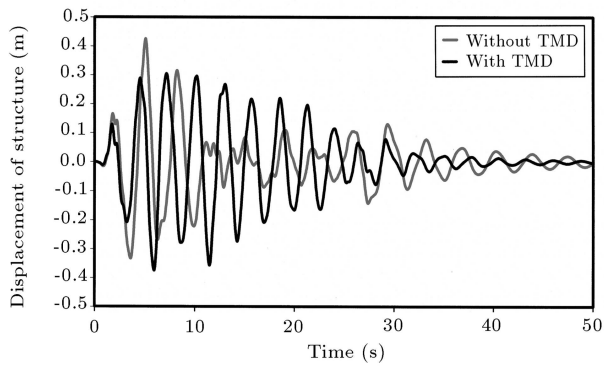
(b) 8-story structure



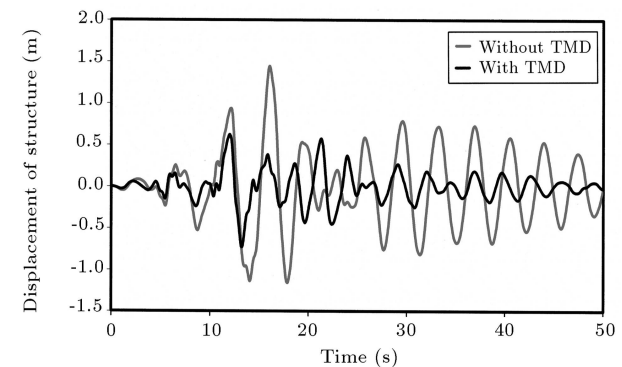
(c) 10-story structure



(c) 10-story structure



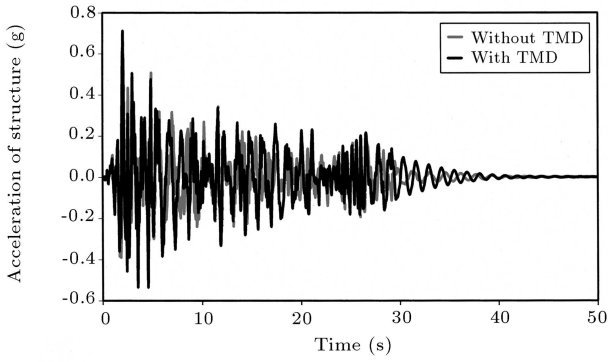
(d) 15-story structure



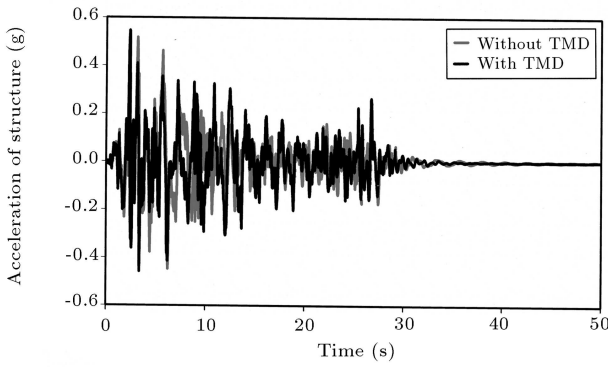
(d) 15-story structure

Figure 8. Displacement of structures with and without TMD under the El Centro earthquake.

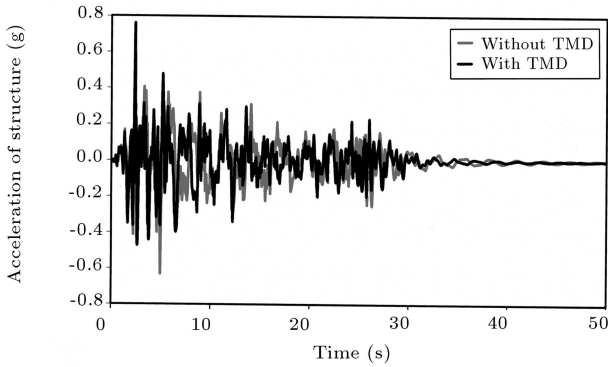
Figure 9. Displacement of structures with and without TMD under the Tabas earthquake.



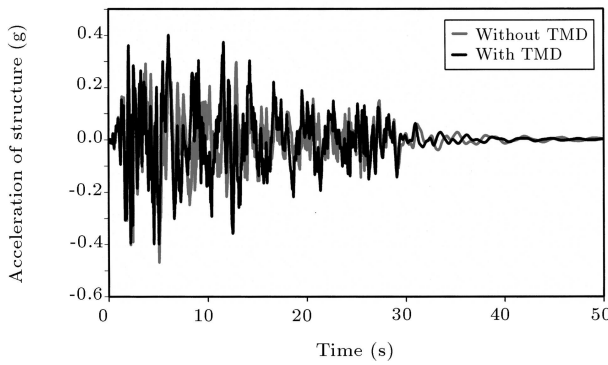
(a) 5-story structure



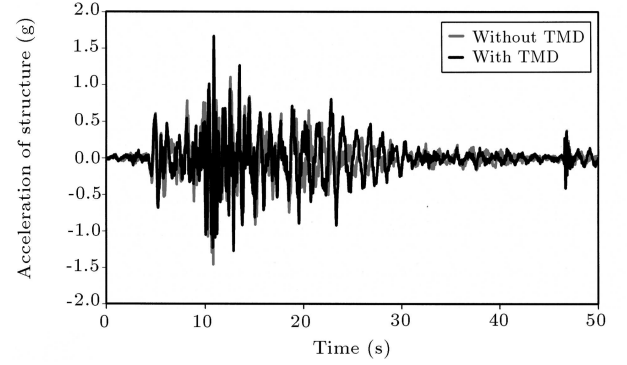
(b) 8-story structure



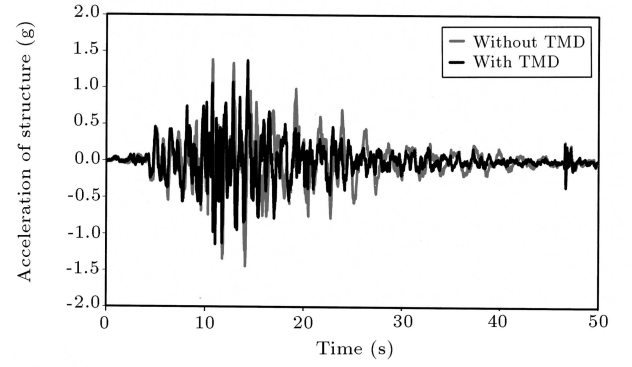
(c) 10-story structure



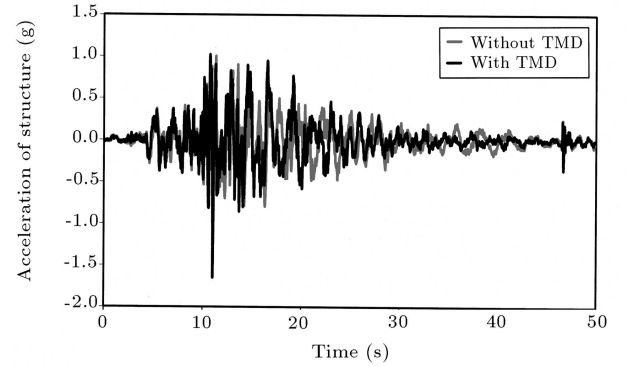
(d) 15-story structure

Figure 10. Acceleration of structures with and without TMD under the El Centro earthquake.

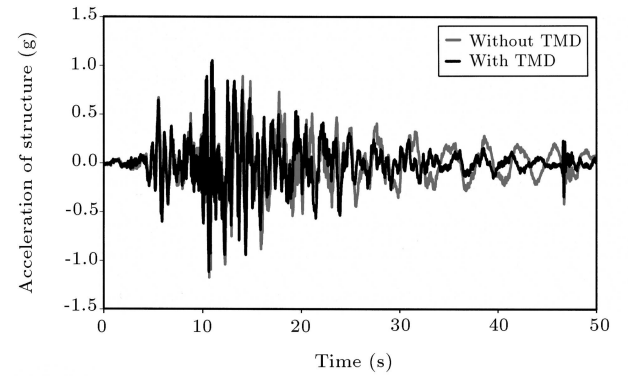
(a) 5-story structure



(b) 8-story structure



(c) 10-story structure



(d) 15-story structure

Figure 11. Acceleration of structures with and without TMD under the Tabas earthquake.

Table 4. RMS values of the accelerations of the structures.

Structures	Accelerations Under the Tabas (g)			Accelerations Under the El Centro (g)		
	Uncontrolled	Controlled	R	Uncontrolled	Controlled	R
5-Story	0.23507	0.26046	1.10801	0.09691	0.11271	1.16301
8-Story	0.26702	0.23280	0.87184	0.09197	0.09310	1.01220
10-Story	0.19848	0.21509	1.08369	0.10527	0.09663	0.91794
15-Story	0.23299	0.20847	0.89475	0.08080	0.09581	1.18570

Table 5. Max values of the accelerations of the structures.

Structures	Accelerations Under the Tabas (g)		Accelerations Under the El Centro (g)	
	Uncontrolled	Controlled	Uncontrolled	Controlled
5-Story	1.53257	1.66108	0.65674	0.71140
8-Story	1.43960	1.37129	0.54194	0.54636
10-Story	1.49225	1.62447	0.69006	0.75570
15-Story	1.17231	1.10366	0.46759	0.39977

To clearly demonstrate the passive control effectiveness, a control performance index is defined, as follows:

$$R = \frac{\langle u \rangle_{\text{controlled case}}}{\langle u \rangle_{\text{uncontrolled case}}},$$

where $\langle u \rangle_{\text{controlled case}}$ denotes the RMS value of the displacement (or acceleration) of the controlled case and $\langle u \rangle_{\text{uncontrolled case}}$ denotes the RMS value of the displacement (or acceleration) of the uncontrolled case. From Table 4, it is obvious that TMD reduces the average acceleration. Table 5 shows the maximum acceleration time-histories of structures with and without TMD under the El Centro and Tabas earthquakes. From Table 5 and Figure 10d, it is demonstrated that, in a 15-story structure, the maximum acceleration of the uncontrolled case, under the El Centro earthquake, is 0.468 g and that of the controlled case is 0.399 g. In comparison with a 15-story structure, in a 10-story structure, the maximum acceleration of the uncontrolled case under the El Centro earthquake is 0.690 g, while that of the controlled case is 0.756 g, showing the lack of efficiency of TMD in mitigated seismic excitation.

The result shows that the maximum acceleration of the uncontrolled case under the Tabas earthquake is 1.492 g and that of the controlled case is 1.624 g, in a 10-story structure. On the other hand, in an 8-story structure, the maximum acceleration of the uncontrolled case under the Tabas earthquake is 1.439 g, while that of the controlled case is 1.371 g (Figure 11c). As presented by numerical results, a single TMD can only control the mode for which it is designed. Therefore, the concept of Multi-Tuned Mass Dampers (MTMD), i.e., having a separate TMD for other structural modes, appears to be a solution

to the limited efficiency of TMD in mitigating seismic vibrations. The application of an active mass damper can also be considered as an alternative, to suppress the effects of higher modes of vibration for important high-rise structures.

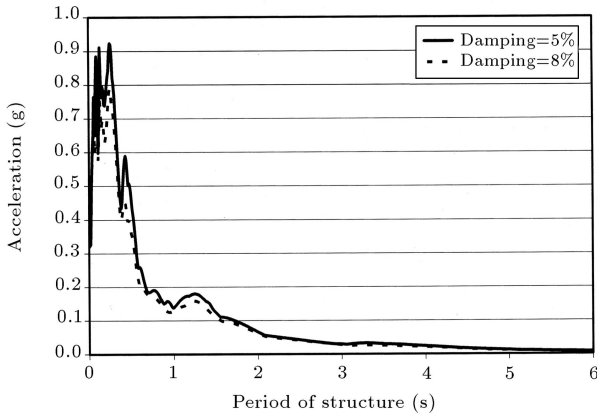
In order to judge about the effectiveness of the TMD in this study, the results of a time-history analysis are compared with the results of a response spectrum analysis for the structures with and without TMD. A response spectrum analysis is currently the most popular method of dynamic response analysis. Response spectrum representation can either be elastic or inelastic; whereas an inelastic spectrum can be either constant strength or constant ductility [21]. It is apparent that use of the response spectrum method has limitations, some of which can be removed by additional development. However, it will never be accurate for nonlinear analysis of multi-degree of freedom structures. Hence, researchers believe that, in the future, more time-history dynamic response analyses will be conducted and the many approximations associated with the use of the response spectrum method will be avoided [22].

The response spectrum method allows an approximate determination of the maximum response of a MDOF system, without performing a time-history analysis. A response spectrum analysis consists of three steps:

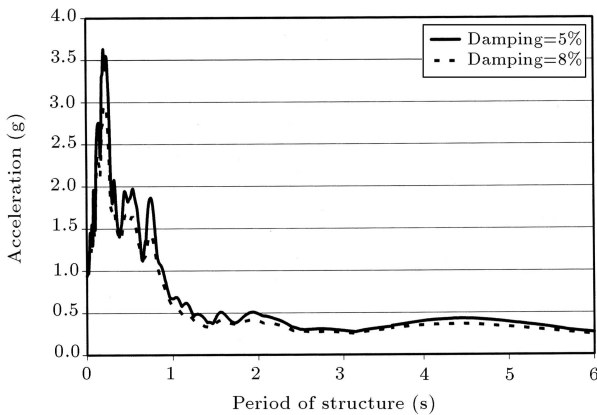
1. Determination of the natural modes of vibration,
2. Determination of the maximum response in each mode,
3. Combination of the modal responses by the SRSS (Square Root Sum of Squares) rule to obtain approximate maximum response [23].

The requirement that all significant modes, as determined from analysis and presented in Table 1, should be included in the response analysis, may be satisfied by including sufficient modes to capture at least 90% of the participating mass of the building in each principal horizontal direction of the building.

Response spectrum analyses of structures were conducted using selected earthquake record spectrums, presented in Figures 12 and 13, with modal information presented in Table 1 and above the proposed analysis steps. For example, by referring to the response spectrum analysis, the maximum response of the uncontrolled case is 13.32 cm and that of the controlled case is 11.58 cm, in a 5-story structure in the El Centro earthquake. But, by using time-history analysis, the maximum response of the uncontrolled case is 14.04 cm and that of the controlled case is 11.78 cm. Compared to a 5-story structure, the maximum displacements, using a response spectrum analysis for the uncontrolled and controlled cases in the El Centro earthquake, are 25.70 cm and 14.59 cm, respectively, in an 8-story structure. However, the maximum displacement,

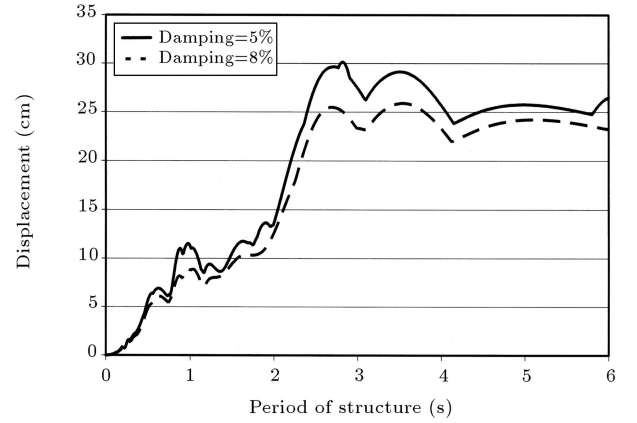


(a) Structures under the El Centro earthquake

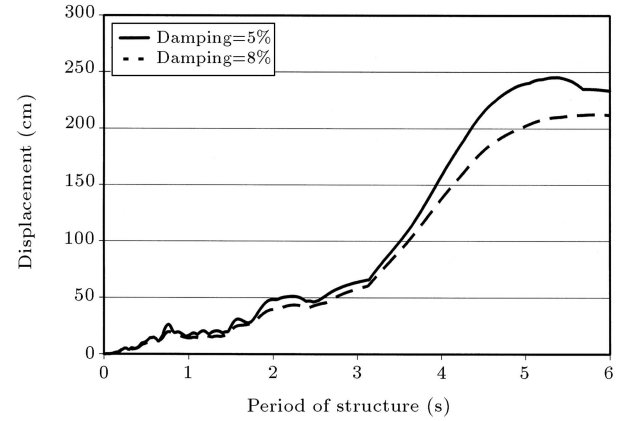


(b) Structures under the Tabas earthquake

Figure 12. Acceleration response spectrum of the El Centro and Tabas records.



(a) Structures under the El Centro earthquake



(b) Structures under the Tabas earthquake

Figure 13. Displacement response spectrum of the El Centro and Tabas records.

using time-history analysis for the uncontrolled and controlled cases, is 27.54 cm and 15.14 cm, respectively.

By referring to response spectrum analysis, in a 10-story structure in the Tabas earthquake, the maximum response of the uncontrolled case is 71.98 cm and that of the controlled case is 52.11 cm. But, by using time-history analysis, the maximum displacement of the uncontrolled case is 80.85 cm and that of the controlled case is 57.91 cm. The difference between the maximum displacement values resulted by the two methods discussed above, is mainly due to the number of modes involved.

Also, using response spectrum analysis, maximum acceleration of the uncontrolled case is 0.465 g and that of the controlled case is 0.391 g, in a 15-story structure under the El Centro earthquake. However using a time-history analysis, the maximum acceleration of the uncontrolled case is 0.467 g and that of the controlled case is 0.399 g. By referring to the response spectrum analysis, in an 8-story structure in the Tabas earthquake, maximum acceleration of the

uncontrolled case is 1.362 g and that of the controlled case is 1.329 g. On the other hand, the maximum acceleration, using time-history analysis, for the uncontrolled and controlled cases, is 1.439 g and 1.371 g, respectively. Thus, there is no significant difference between maximum acceleration values determined by the two aforementioned methods.

CONCLUSIONS

Based on the numerical results obtained in this paper, overall, TMD is effective in reducing displacement and average acceleration and, thereby, can be used as an effective control measure for structures under earthquake. In this study, the effectiveness of the TMD controlling the 5-, 8-, 10- and 15-story buildings, subjected to both the El Centro and Tabas earthquakes, is investigated. In the time-history analysis, using the El Centro and Tabas earthquakes, the TMD parameters designed for harmonic excitations were observed to be performing close to the best possible. The numerical results showed that the amplitude of structural displacement having TMD is considerably lower than the displacements of the same structure without any control mechanisms. For example, TMD reduced maximum displacement in MRF buildings by as much as a maximum of 32.2% in the Tabas earthquake and a maximum of 45.3% in the El Centro earthquake. In order to judge the effectiveness of TMD in this study, the results of the time-history analysis are compared with the results of the response spectrum analysis for the structures with and without TMD. For example, in a 10-story structure in the Tabas earthquake, the maximum response of the uncontrolled case is 71.98 cm and that of the controlled case is 52.11 cm. But, by the time-history analysis, the maximum response of the uncontrolled case is 80.85 cm and that of the controlled case is 57.91 cm. The slight difference between the maximum displacement values resulted by the two methods is mainly due to the number of modes involved in each.

Finally, based on findings in this study, when the first mode of a MRF building dominates the structural response, a response reduction of the MRF building, using TMD under earthquake loading, can be achieved. On the other hand, based on the numerical results showed in this paper, the response reduction is large for resonant ground motions, which decreased as the dominant frequency of the ground motion got further away from the structure's natural frequency to which the TMD is tuned. Therefore, it can be seen that the effect of ground motion parameters, namely; intensity of ground motion, central frequency, bandwidth of ground motion, duration of strong motion on the seismic effectiveness of TMD and its optimum parameters, may be a problem, which needs further study. In addition, the

diminution of the maximum displacement of structures weakens with an enhancement story number, which also needs more study.

REFERENCES

1. Lin, C.C., Ueng, J.M. and Huang, T.C. "Seismic response reduction of irregular buildings using passive tuned mass dampers", *Engineering Structures*, **22**, pp 513-524 (1999).
2. Pinkaew, T., Lukkunaprasit, P. and Chatupote, P. "Seismic effectiveness of tuned mass dampers for damage reduction of structure", *Engineering Structures*, **25**(1), pp 39-46 (2003).
3. Rana, R. and Soong, T.T. "Parametric study and simplified design of tuned mass dampers", *Engineering Structures*, **20**(3), pp 193-204 (1998).
4. ENR "Hancock tower now to get dampers", *Engineering News-Records*, McGraw-Hill, pp 11-13 (1975).
5. Kwok, K.C.S. "Damping increase in building with tuned mass damper", *J. Eng. Mech., ASCE*, **110**(11), pp 1645-1649 (1984).
6. Soong, T.T. and Dargush, G.F., *Passive Energy Dissipation Systems in Structural Engineering*, John Wiley & Sons, New York (1997).
7. Ormondroyd, J. and Den Hartog, J.P. "The theory of dynamic vibration absorber", *Trans. ASME*, **50**(7), pp 9-22 (1928).
8. Bishop, R.E.D. and Welbourn, D.B. "The problem of the dynamic vibration absorber", *Engineering*, London, pp 174-769 (1952).
9. Snowdown, J.C. "Steady-state behavior of tile dynamic absorber", *Jacobs. Soc. Am.*, **31**(8), pp 1096-1103 (1960).
10. Falcon, K.C., Stone, B.J., Simcock, W.D. and Andrew, C. "Optimization of vibration absorbers: A graphical method for use on idealized systems with restricted damping", *J. Mech. Engng. Sci.*, **9**, pp 374-381 (1967).
11. Ioi, T. and Ikeda, K. "On the dynamic vibration damped absorber of the vibration system", *Bulletin Japanese Society of Mechanical Engineering*, **21**(151), pp 64-71 (1978).
12. Warburton, G.B. and Ayorinde, E.O. "Optimum absorber parameters for simple systems", *Earthquake Engineering and Structural Dynamics*, **8**, pp 197-217 (1980).
13. Thompson, A.G. "Optimum damping and tuning of a dynamic vibration absorber applied to a force excited and damped primary system", *J. Sound Vib.*, **77**, pp 403-415 (1981).
14. Warburton, G.B. "Optimal absorber parameters for various combinations of response and excitation parameters", *Earthq. Engng. Struct. Dyn.*, **10**, pp 381-401 (1982).
15. Vickery, B.J., Isyumov, N. and Davenport, A.G. "The role of damping, mass and acceleration", *Wind Engng Ind. Aerodynam.*, **II**, pp 285-294 (1983).

16. Tsai, H.C. and Lin, G.C. "Optimum tuned mass dampers for minimizing steady-state response of support excited and damped systems", *Earthq. Engng Struct. Dynam.*, **22**, pp 957-973 (1993).
17. Den Hartog, J.P., *Mechanical Vibrations*, 4th Ed, New York, McGraw-Hill (1956).
18. Zahrai, S.M. and Ghannadi-Asl, A. "Seismic response reduction of tall buildings using tuned mass dampers", *7th International Conference on Multi-Purpose High-Rise Towers and Tall Buildings*, Dubai, UAE (2005).
19. Building and Housing research center of Iran "Iranian code of practice for seismic resistant design of buildings", *Standard No. 2800*, 2nd Ed. (1999).
20. Computers and Structures Inc. "ETABS nonlinear version 8.2.7", (2003).
21. Singh, J.P. "Seismic loading: Code versus site specific", *Portland Regional Seminar on Seismic Engineering Issues*, USA (1995).
22. Wilson, E.L., *Three Dimensional Static and Dynamic Analysis of Structures*, Berkeley, California: Computers and Structures Inc. Press (2002).
23. Chen, W.F. and Scawthorn, Ch., *Earthquake Engineering Handbook*, New York, CRC Press (2003).